Applied and Environmental Microbiology, Oct. 2007, p. 6508–6518 Vol. 73, No. 20
0099-2240/07/$08.00+0 doi:10.1128/AEM.01212-07
Copyright © 2007, American Society for Microbiology. All Rights Reserved.

Damage in *Escherichia coli* Cells Treated with a Combination of High Hydrostatic Pressure and Subzero Temperature[▽]

Marwen Moussa, Jean-Marie Perrier-Cornet,* and Patrick Gervais

Laboratoire de Génie des Procédés Microbiologiques et Alimentaires, ENSBANA, Université de Bourgogne, 1, Esplanade Erasme, 21000 Dijon, France

Received 31 May 2007/Accepted 19 August 2007

The relationship between membrane permeability, changes in ultrastructure, and inactivation in *Escherichia coli* strain K-12TG1 cells subjected to high hydrostatic pressure treatment at room and subzero temperatures was studied. Propidium iodide staining performed before and after pressure treatment made it possible to distinguish between reversible and irreversible pressure-mediated cell membrane permeabilization. Changes in cell ultrastructure were studied using transmission electron microscopy (TEM), which showed noticeable condensation of nucleoids and aggregation of cytosolic proteins in cells fixed after decompression. A novel technique used to mix fixation reagents with the cell suspension in situ under high hydrostatic pressure (HHP) and subzero-temperature conditions made it possible to show the partial reversibility of pressure-induced nucleoid condensation. However, based on visual examination of TEM micrographs, protein aggregation did not seem to be reversible. Reversible cell membrane permeabilization was noticeable, particularly for HHP treatments at subzero temperature. A correlation between membrane permeabilization and cell inactivation was established, suggesting different mechanisms at room and subzero temperatures. We propose that the inactivation of *E. coli* cells under combined HHP and subzero temperature occurs mainly during their transiently permeabilized state, whereas HHP inactivation at room temperature is related to a balance of transient and permanent permeabilization. The correlation between TEM results and cell inactivation was not absolute. Further work is required to elucidate the effects of pressure-induced damage on nucleoids and proteins during cell inactivation.

High hydrostatic pressure (HHP) processing is an emerging technology that has stimulated considerable interest in the food industry. HHP can be used alone or in combination with thermal or nonthermal techniques for the inactivation of a wide variety of microorganisms. Combined treatments have been investigated in order to optimize HHP processes to allow large-scale applications in the food industry. The combination of HHP with low and subzero temperatures is an attractive method of process optimization that is compatible with the so-called cold stabilization brand image of HHP-processed foods. Several authors have reported an enhancement of pressure inactivation of various microorganisms at low (17, 36) and subzero (9, 10, 38) temperatures. In the latter studies, cell suspensions were frozen prior to pressurization, perhaps because of difficulties in maintaining the liquid state of aqueous cell suspensions during HHP and subzero-temperature combinations, and the effects of freeze-thaw phenomena or possible solid-solid phase transitions of water molecules under hyperbaric and subzero-temperature conditions were disregarded. Such phase transition phenomena have been reported to enhance the pressure inactivation of *Listeria innocua* cells (18, 30) and *Bacillus subtilis* vegetative cells (32). A very precise control of pressure and temperature is required to detect freezing in the cell suspensions being treated and to ensure pressurization in the liquid state. Recent studies reported pressurization in the liquid state at subzero temperature of yeast *Saccharomyces cerevisiae* (29), of the gram-positive bacterium *Lactobacillus plantarum* (29), and of the gram-negative bacterium *Escherichia coli* (23).

HHP research has been focused primarily on the cellular targets and the mechanisms of HHP-induced microbial inactivation. The cell membrane has been suggested to be one of the major targets (8, 22, 25, 39, 40). Loss of physical integrity of *E. coli* outer and inner membranes has been demonstrated by the increased uptake of fluorescent probes such as propidium iodide (PI), a DNA binding dye that does not penetrate intact cytoplasmic membranes (1, 8, 25), and the hydrophobic dye 1-*N*-phenylnaphtylamine, which is excluded from access to outer and cytoplasmic phospholipids by an intact outer membrane (8, 13). Pressure-mediated thermotropic changes in membrane lipids have been suggested as a possible mechanism of membrane permeabilization (19, 28). Perrier-Cornet et al. (27) related pressure-induced shape modifications of phospholipid vesicles to phase transition and differential compression rates of intravesicle bulk water and the vesicle membrane. Furthermore, the phase transition of a lipid bilayer from the liquid crystalline phase to a gel phase would be expected to alter the environment of membrane-bound proteins (11). This phenomenon could induce the loss of membrane functionality described by several authors (15, 31, 40, 41). Ribosomes and cytoplasmic proteins could also be affected by pressure (24). Transmission electron microscopy (TEM) offers the attractive possibility of identifying such structural changes in microorganisms. TEM studies by Mackey et al. (21) of the pressure-induced structural changes in *Listeria monocytogenes* and *Salmonella enterica* serovar Thompson showed enlarged fibrillar

* Corresponding author. Mailing address: Laboratoire de Génie des Procédés Microbiologiques et Alimentaires, ENSBANA, Université de Bourgogne, 1, Esplanade Erasme, 21000 Dijon, France. Phone: 33 3 80 39 68 45. Fax: 33 3 80 39 68 98. E-mail: jperrier@u-bourgogne.fr.
▽ Published ahead of print on 31 August 2007.

regions and amorphous compacted regions. These observations have been assumed to be due, respectively, to denatured DNA and to cytoplasmic proteins. Similar observations have been reported by Park et al. (26) and Kaletunç et al. (14).

Taken together, the above observations have led to the proposal of several hypotheses about the mechanisms of HHP inactivation of microorganisms. However, the distinctive effects on the membrane integrity and ultrastructure of cells of combined HHP and subzero-temperature treatments have not been thoroughly characterized. Furthermore, there remains a major unanswered question about the reversibility of these effects.

This work aimed to investigate the mechanisms leading to cell inactivation by HHP treatment and to study whether there are different targets at room and subzero temperatures. The study was focused on an assessment of membrane permeabilization and changes in the ultrastructure in *E. coli* K-12TG1 cells and on the relationship of these parameters to cell inactivation. Reversible and irreversible loss of cell membrane integrity was assessed using PI staining. In order to examine the exact state of *E. coli* cells under pressure and assess the possible reversibility of the ultrastructural changes, a novel technique was developed to mix fixation reagents with the cell suspension in situ under HHP and subzero-temperature conditions.

MATERIALS AND METHODS

Bacterial strain and growth conditions. A stock culture of *E. coli* K-12TG1 [*supE hsd*Δ*5 thi*Δ(*lac-proAB*)F′ (*traD36 proAB lacI*^{q} *lacZ*Δ*M15*)] was maintained on Luria-Bertani (LB) stock agar plates (Sigma Aldrich, France). *E. coli* was subcultured by transferring a single colony from the stock plate to an autoclaved test tube containing 9 ml of LB broth at a pH of approximately 6.7 (not adjusted). This tube was then incubated statically for 16 h at 37°C. The *E. coli* culture was inoculated (1% [vol/vol]) into 20 ml of LB broth, and this was grown statically at 37°C for 24 h until it reached stationary phase.

HHP treatments. (i) Sample preparation. Samples of approximately 800 μl of *E. coli* culture were transferred aseptically to polyethylene bags (Samco) that were heat sealed after the exclusion of air bubbles. Samples were then placed at room temperature and pressure until pressurization. The final cell concentration ranged from 4×10^8 to 8×10^8 CFU ml^{-1}.

(ii) HHP experimental setup. HHP treatments were performed using a high-pressure vessel (Laboratoire d'Ingénierie des Matériaux et des Hautes Pressions, France) of a 40-mm outside diameter, a 7-mm inside diameter, an 86-mm height, and a 60-mm depth. This vessel had an inner volume of 4 ml and was capable of operating at up to 600 MPa. Pressure was generated using a hand pump (Novaswiss, Switzerland). Ethanol was chosen as the pressure-transmitting fluid based on its low freezing point. The pressure inside the sample chamber was monitored using a pressure gauge (Sedeme, France). The temperature was measured using a type K thermocouple (NiCr/NiAl, response time of 70 ms; Thermocoax, France) positioned close to the sample. Pressure and temperature data were recorded using a data acquisition device (instruNet; GW Instruments). The global accuracy of each acquisition channel was approximately 0.5°C for temperature and 0.5% for pressure.

(iii) High-pressure treatment at +25°C. HHP of up to 550 MPa was applied to the bacterial samples. The pressure was increased slowly by operating the hand pump. The temperature was maintained at +25°C by immersing the high-pressure vessel in a temperature-controlled water bath. Compression heat was minimal (less than +2°C) at all pressure targets, and this was rapidly dissipated due to the low compression rate and the temperature-controlled water bath. Treatment time was measured from the time immediately after the target pressure was reached. Pressure was then held constant for 10 min before the decompression phase was initiated. The ramp-up and ramp-down times were 2 min 30 s regardless of the target pressure. For treatments with a 0-min holding time, decompression was initiated immediately after the pressure ramp-up to 250 MPa.

(iv) HHP treatments at −10 and −20°C in liquid conditions. Combined high-pressure and subzero-temperature treatments were performed as described previously (23). Two cryostats loaded with 95% ethanol as the circulating fluid were used consecutively to lower the temperature of the HHP vessel. For treatments performed at −10°C, the first cryostat (F81-HP; Julabo, Germany) was maintained at −30°C in order to accelerate heat transfer. The HHP vessel was first immersed in this cryostat until the temperature of the sample chamber reached +2°C and then transferred into a second cryostat (RC6CP; Lauda, Germany) maintained at −10°C in order to hold a constant temperature during the treatment process. For treatments performed at −20°C, the first cryostat was maintained at −60°C, and the HHP vessel was transferred into the second cryostat maintained at −20°C as soon as the temperature inside the sample chamber reached 0°C. Pressure was increased while the temperature was lowered in a manner to reach pressure and temperature targets at approximately the same time. After the required holding time (10 min) at the appropriate temperature and pressure, the HHP vessel was reheated by immersion in a water bath maintained at +27°C. Pressure was simultaneously released by slowly operating the hand pump in a manner to reach ambient pressure and temperature at approximately the same time.

Pressure treatments at subzero temperature were performed under liquid conditions whatever the pressure and temperature levels. Indeed, precise pressure and temperature monitoring made it possible to identify possible liquid-to-ice I, -ice III, and -ice V phase transitions (23).

Enumeration of viable *E. coli* cells. HHP-treated samples were serially diluted, and appropriate dilutions were then plated onto LB agar plates. These were incubated for 22 h at +37°C, after which CFU were counted. The microbial inactivation achieved with each treatment was expressed as the logarithmic decrease in viability according to the following equation: $\mathrm{Dlog} = \log_{10}(n/n_0)$, where n is the number of CFU ml^{-1} after treatment and n_0 is the number of CFU ml^{-1} from the untreated sample. Results are reported as the means of three to six separate experiments.

The 95% confidence intervals of the means were determined based on n/n_0 quotient calculations. Student's t test was performed to determine the statistical significance ($P < 0.05$) of differences between the inactivation data.

Cell staining and epifluorescence microscopic imaging. (i) Assessment of reversible and irreversible cell membrane permeability to PI. Cell membrane permeability was assessed using PI staining. A 1.5 mM stock solution of PI (Sigma Aldrich, France) in water was diluted with sterile distilled water to a concentration of 0.3 mM. Pressure-treated samples of *E. coli* were stained with PI added to a final concentration of 75 μM. After incubation for 15 min, the samples were centrifuged twice at 2,880 × *g* and washed in a water-glycerol mixture (44.88 g of glycerol [Sigma Aldrich, France] in 1,000 g of water; osmotic pressure of approximately 1.38 MPa).

A modified procedure of cell staining with PI was used in order to assess the reversibility of cell membrane permeabilization. PI was added to the cell suspension before HHP treatment at a final concentration of 75 μM. After pressure treatment, the samples were centrifuged and washed as described above.

For both procedures, samples were examined under an inverted Nikon TE2000-E microscope (Nikon Corporation, France) equipped with a Nuance multispectral imaging system (Cambridge Research & Instrumentation). A 100× objective was used with a total magnification of ×1,000. Black-and-white images were captured to show the total cell population. A monochromatic epifilter (540- to 580-nm and 600- to 660-nm excitation and emission wavelengths, respectively) was used, and color images were captured to show only cells exhibiting red fluorescence from DNA labeling with PI as a result of membrane permeabilization.

The cell membrane permeabilization achieved with each treatment was expressed as the percentage of red fluorescent cells compared to total cell counts for the black-and-white images (at least 300 cells). Red fluorescent cells labeled with PI added after decompression were considered as irreversibly permeabilized. The percentage of reversible cell membrane permeabilization was calculated as the difference between the percentage of irreversibly permeabilized cells and the percentage of red cells obtained when PI was added before treatment. The 95% confidence intervals of the means were determined, and Student's t test was performed to determine statistical significance ($P < 0.05$).

(ii) Staining cellular nucleoids and proteins. Cellular nucleoids were visualized in treated samples by staining with 100 μM 4′,6′-diamidino-2-phenylindole (DAPI) (Sigma Aldrich, France). A 130 μM solution of fluorescein isothiocyanate (FITC) (Sigma Aldrich, France) was used to stain cellular proteins of treated samples. For both DAPI and FITC staining, samples were incubated for 15 min, centrifuged, and washed as described above. Microscopic imaging was then performed as described above using epifluorescence light with the appropriate monochromatic filter as follows: 340-to 380-nm excitation and 435- to

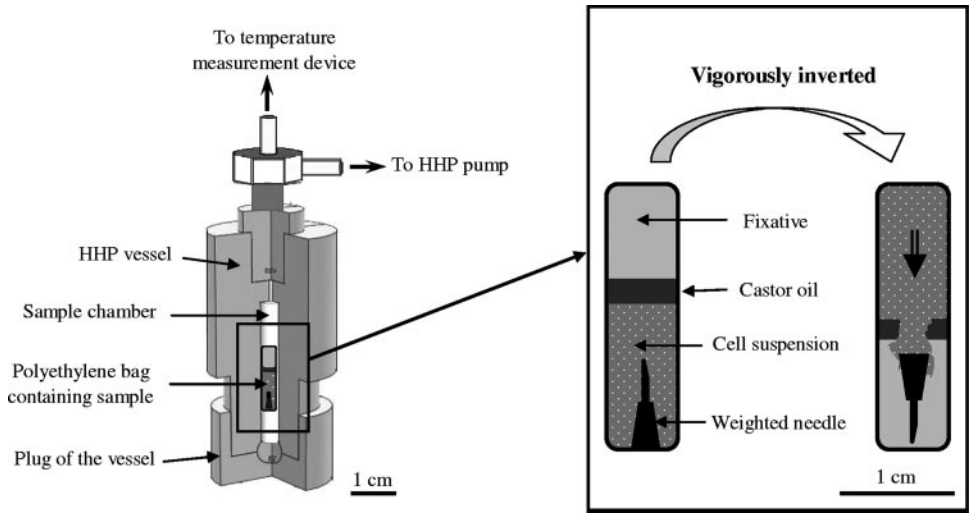

FIG. 1. Technique for cell fixation in situ under combined HHP and subzero-temperature conditions. Three-quarters cross section of the HHP vessel containing a sample. The vessel was vigorously inverted to allow the cell suspension to mix with the fixative solution.

485-nm emission wavelengths for DAPI staining and 460- to 500-nm excitation and 510- to 560-nm emission wavelengths for FITC staining.

TEM. (i) Fixation after decompression. After the HHP treatments, both the treated and the untreated samples were immediately mixed with a fixative solution (4% paraformaldehyde and 1.5% glutaraldehyde in 100 mM phosphate buffer, pH 7.4; Merck, France) for 30 min at room temperature. The cells were then pelleted by centrifugation (2,880 × *g* for 5 min at +25°C), and the supernatant was discarded. The cell pellets were resuspended in phosphate buffer and pelleted as before, and the process was repeated twice more to remove excess fixative. Samples were then transferred to the Laboratory of Histology of the Faculty of Medicine (Université de Bourgogne, France). There, the cells were postfixed in 1% osmium tetroxide (Euromedex, France) for 1 h in darkness at room temperature. Afterward, cells were dehydrated in increasing concentrations of ethanol as follows: in 30%, in 50%, in 70%, in 95%, and three times in 100% for 15 min each. Then, cells were transferred to three consecutive baths of propylene oxide (Merck, France) for 15 min each. Samples were then embedded in EPOX 812 resin and finally polymerized at +60°C for 48 h. Ultrathin sections (80 nm) were cut on an ultramicrotome, placed on a 200-mesh copper-palladium grid, and stained with 5% uranyl acetate (Merck, France) in order to improve contrast. Grids were examined at 80 kV in a Hitachi 7500 TEM equipped with a camera and specific software (Advanced Microscopy Techniques) allowing digitization of TEM micrographs.

(ii) Technique for cell fixation under HHP and subzero conditions. In order to examine the state of *E. coli* cells under pressure and to assess the possible reversibility of ultrastructural changes, a special technique was devised to mix fixation reagents with the cell suspension under HHP and subzero-temperature conditions (Fig. 1). A 600-μl sample of *E. coli* culture was transferred aseptically to a transfer pipette and a weighted needle was immersed in the sample before a thin layer of castor oil was carefully placed over the sample. Finally, the fixative solution (400 μl of the paraformaldehyde-glutaraldehyde mixture) was placed over the castor oil layer. The transfer pipette was heat sealed at the upper side and placed inside the HHP sample chamber. The HHP vessel was then tightly closed and connected to the pump. Pressurization was then performed as described above. *E. coli* cells were fixed under pressure by vigorously inverting the vessel, allowing the cell suspension and fixative solution to mix. The effectiveness of the weighted needle in breaking the castor oil layer was verified using a fixative solution stained with a dye visible to the naked eye. This fixation procedure was used to fix cells under hyperbaric conditions (250 MPa at +25°C and −20°C) after 0- and 10-min holding times. The fixed cells were postfixed and embedded, and the ultrathin sections were prepared as described above.

(iii) Examination of TEM micrographs. The structural changes observed for *E. coli* sections were quantified by examining a number of micrographs for each treatment. The percentage of affected cells was calculated with respect to the total number of cells examined (at least 300) for each micrograph.

RESULTS

Inactivation of *E. coli* cells by HHP treatment at room and subzero temperatures. *E. coli* cells were exposed to pressure treatments of up to 550 MPa at −20°C, −10°C, and +25°C for 10 min. Figure 2 shows the logarithmic decrease in the viability of *E. coli* cells as a function of pressure and temperature. Pressure of 150 MPa did not induce a significant loss of viability at +25°C. However, it induced a 1.5-log unit inactivation at −10°C and −20°C. This enhancement of *E. coli* inactivation at subzero temperature was also noticeable at 250 MPa. Indeed, the rate of inactivation was approximately 2.3 log units higher at −10°C and −20°C than at +25°C. The gap between inactivation rates at room and subzero temperatures was reduced at 350 MPa. This trend resulted from the consistent increase of microbial inactivation at +25°C and its slow progression at −10°C and −20°C. At 450 and 550 MPa, *E. coli* inactivation at −10°C and −20°C leveled off, although it was consistently increased at +25°C. Accordingly, the complete inactivation of the initial cell population was achieved at 550 MPa and +25°C, while inactivation did not exceed 4.7 log units at −10°C and −20°C. Thus, the synergy between subzero temperature and HHP observed at 150 and 250 MPa was completely reversed at 450 and 550 MPa, and microbial inactivation was higher at +25°C than at −10°C and −20°C.

The different behaviors with regard to pressurization at room and subzero temperatures shown by *E. coli* strain K-12TG1 were also observed for strain LCB 320 (data not shown).

HHP-mediated permeabilization at room and subzero temperatures. Figure 3 shows the levels of irreversible and reversible cell membrane permeability as a function of the pressure level at +25°C and −20°C. Irreversible cell membrane permeability to PI was determined by staining cells after HHP treatments. When PI was present in the suspending medium during treatment, more cells took up the dye than when PI was added after decompression. The difference between the percents

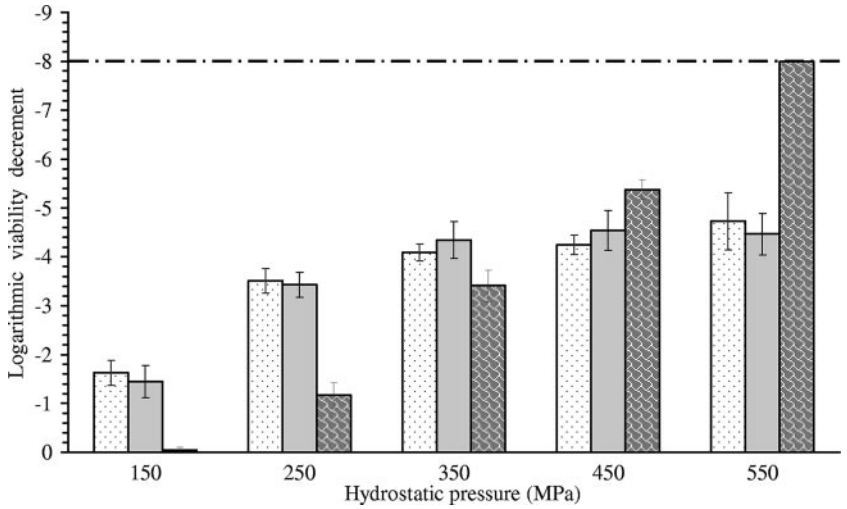

FIG. 2. Inactivation of *E. coli* K-12TG1 after 10-min HHP treatment at −20°C (dotted), −10°C (gray), and +25°C (patterned). The dashed line shows the limit of detection of the CFU count.

staining under the two conditions was defined as the degree of reversible membrane permeabilization to PI.

Exposure of *E. coli* cells to 150 MPa at −20°C induced 35% reversible permeabilization and 9% irreversible permeabilization, whereas at +25°C only a low level of irreversible permeabilization was induced (4%). The percentage of reversible membrane permeabilization at −20°C increased slightly at 250 MPa and then again at 350 MPa and leveled off at 450 and 550 MPa. The same tendency was observed for irreversible permeabilization at −20°C, which increased up to 17% at 350 MPa and then leveled off. Treatments at +25°C and 250 to 450 MPa induced similar degrees of reversible and irreversible permeabilization. HHP-mediated permeabilization to PI was highest at 550 MPa and +25°C. For this treatment, reversible permeabilization seemed to decrease slightly in favor of irreversible permeabilization. In addition, membrane permeability did not reach 100%, as observed for heat treatment (90°C for 10 min), although in both cases microbial inactivation was complete. Similar observations have been reported for *Lactobacillus rhamnosus* GG (1). This indicates that the mechanisms of cell injury by pressure and heat are markedly different.

Changes in the ultrastructure of *E. coli* after HHP treatment at room and subzero temperatures. *E. coli* cells were collected before and after being exposed to a selected set of HHP treatments. Thin sections of fixed and embedded cells were prepared and examined using TEM. Micrographs are presented in Fig. 4. Untreated control cells displayed a uniform cytosol and evenly distributed electron-transparent regions representing bacterial nucleoids (Fig. 4E). Moreover, epifluorescence micrographs of control cells stained with DAPI and FITC showed evenly distributed fluorescence inside the cytoplasm (Fig. 5A and B). HHP treatments induced spectacular changes in the

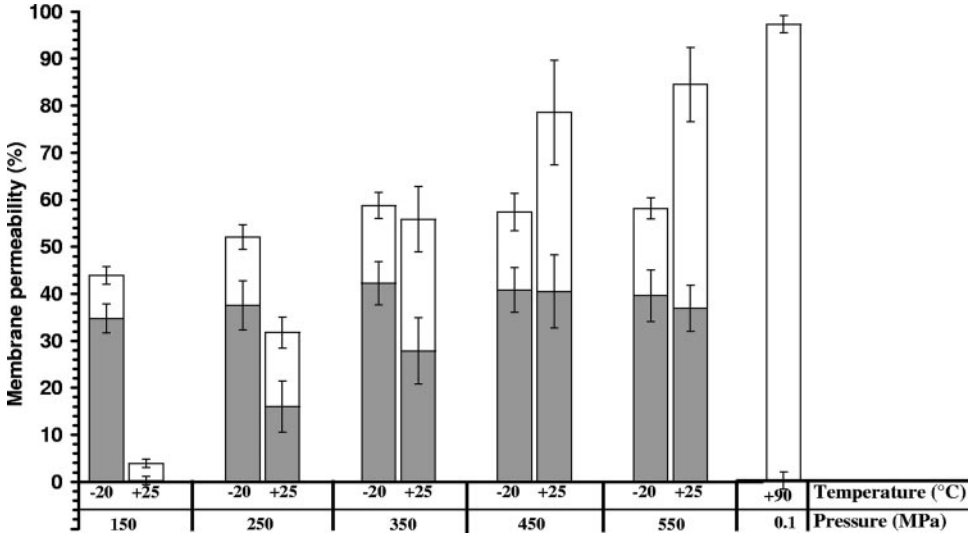

FIG. 3. Reversible (gray portion) and irreversible (white portion) membrane permeabilization of *E. coli* K-12TG1 by 10-min HHP treatments at −20°C and +25°C. Heat-induced permeabilization by a 10-min treatment at +90°C is shown for comparison.

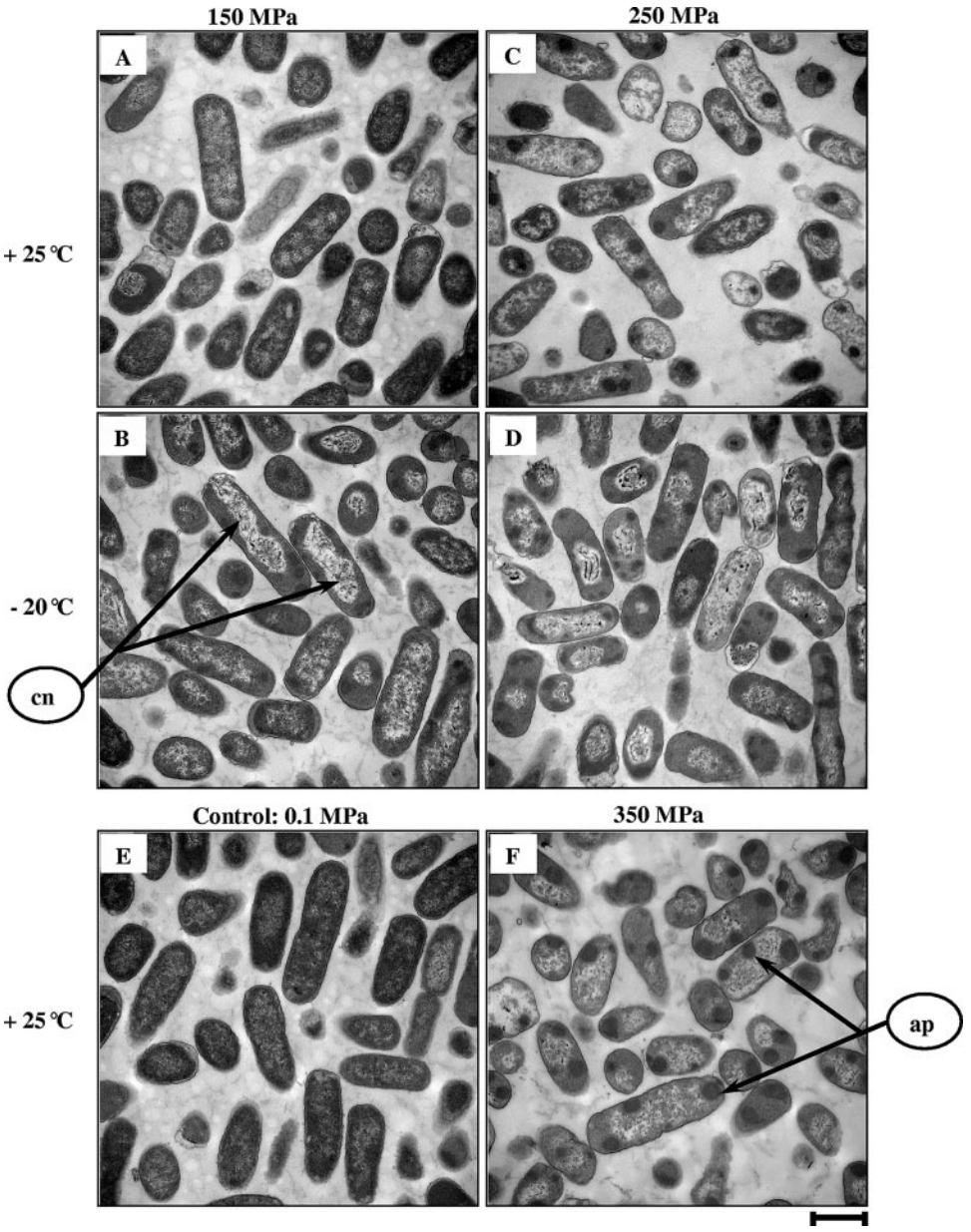

FIG. 4. TEM micrographs of *E. coli* K-12TG1 cells fixed after 10-min HHP treatment. (A to D) Cells treated at 150 MPa and +25°C (A), 150 MPa and −20°C (B), 250 MPa and +25°C (C), and 250 MPa and −20°C (D). (E) Untreated cells. (F) Cells treated at 350 MPa and +25°C. Scale bar, 1 μm. Arrows show condensed nucleoids (cn) and aggregated proteins (ap).

conformation of nucleoids and cytosolic proteins, as revealed by epifluorescence microscopy. For example, Fig. 5C and D show results of a 10-min treatment at 250 MPa and −20°C. Table 1 shows that these structural changes were observed to various extents depending on the treatment. Indeed, the exposure of cells to 150 MPa pressure for 10 min at +25°C induced a slight increase in transparency within the nucleoid regions (Fig. 4A). For the same pressure level, the combination with −20°C caused condensation of the nucleoids in 78% of the cells and the appearance of some clumps of aggregated protein within 45% of the cells (Fig. 4B). TEM micrographs of 250-MPa treatments at +25°C and −20°C for 10 min displayed a proportion of cells with condensed nucleoids and aggregated proteins higher than that seen for treatment at 150 MPa (Fig. 4C and D). Both the intensity and the frequency of protein aggregates within the cell cytoplasm were accentuated after treatment at 350 MPa and +25°C (Fig. 4F). Epifluorescence micrographs of pressure-treated cells at 450 to 550 MPa at +25°C and 350 to 550 MPa at −20°C show approximately the same extents of nucleoid condensation and protein aggregation (more than 95% condensation/aggregation; data not shown).

Kinetics and reversibility of nucleoid condensation and protein aggregation. Studying the kinetics and reversibility of protein aggregation and nucleoid condensation could be a promising avenue to better understand the involvement of such

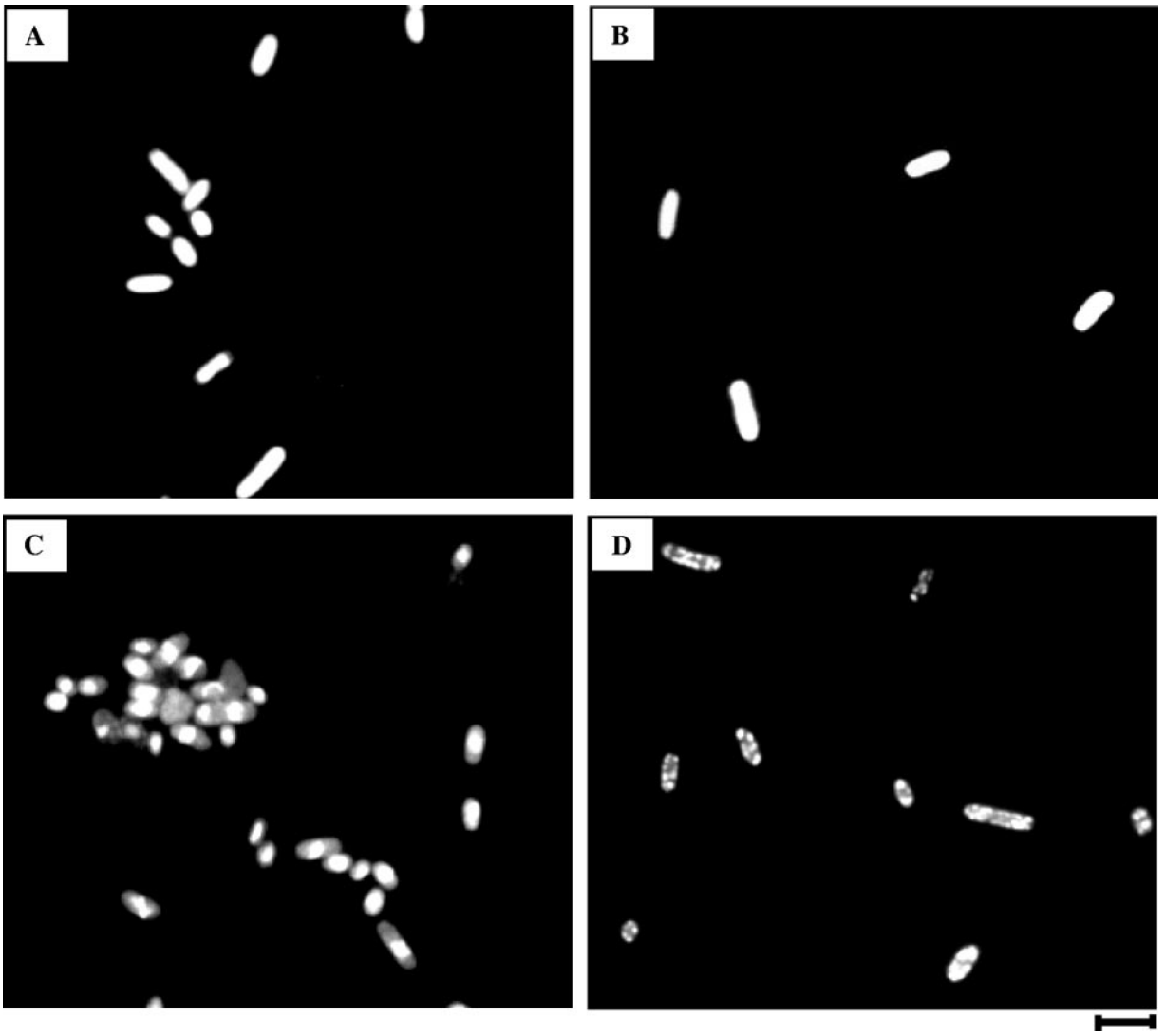

FIG. 5. Epifluorescence micrographs of *E. coli* K-12TG1 cells stained with DAPI and FITC. (A and B) Untreated cells stained with DAPI (A) and FITC (B). (C and D) Cells stained after 10-min treatment at 250 MPa and −20°C with DAPI (C) and FITC (D). Scale bar, 2 μm.

structural changes in the mechanisms of cell inactivation. Figure 6 shows micrographs of *E. coli* cells fixed under HHP conditions at +25°C and −20°C. Cell fixation was performed after 0- and 10-min holding times. Details of this fixation procedure are given in Materials and Methods and diagrammatically presented in Fig. 1. Untreated control cells were fixed using the same procedure as that for treated cells (micrograph not shown) and displayed the same appearance, as shown in Fig. 4E. Table 2 shows that nucleoid condensation occurred within more than 90% of cells as soon as pressure reached 250 MPa at both +25°C (Fig. 6A) and −20°C (Fig. 6C). Nucleoids became progressively more clustered and fibrillar during the holding time at 250 MPa. Protein aggregation seems to be a later event, since it can be observed clearly only after a 10-min treatment at 250 MPa and occurred in 88% of cells at +25°C (Fig. 6B) and in 96% of cells at −20°C (Fig. 6D).

TABLE 1. Structural changes examined by TEM in *E. coli* K12TG1 cells subjected to different HHP treatments for 10 min[a]

Treatment conditions[b]	% of cells with:		% Inactivation (inactivation in Dlog units)
	Condensed nucleoids	Aggregated proteins	
150 MPa at +25°C	10	01	08.80 (−0.04)
150 MPa at −20°C	78	45	97.66 (−1.63)
250 MPa at +25°	83	89	93.24 (−1.17)
250 MPa at −20°C	88	88	99.97 (−3.51)
350 MPa at +25°C	89	94	99.96 (−3.41)

[a] The percentages of affected cells were calculated with respect to the total number of cells examined for each micrograph (at least 300 cells).
[b] Fixation was performed after decompression.

Nucleoid condensation for cells fixed under pressure after a 10-min treatment (Fig. 6C and D) seems slightly more intense than for cells fixed after decompression (Fig. 4B and D). Indeed, condensed nucleoids shown in Fig. 6B to D look slightly more packed and irregularly positioned (often skewed across the cell) than those shown in Fig. 4C and D. This in turn

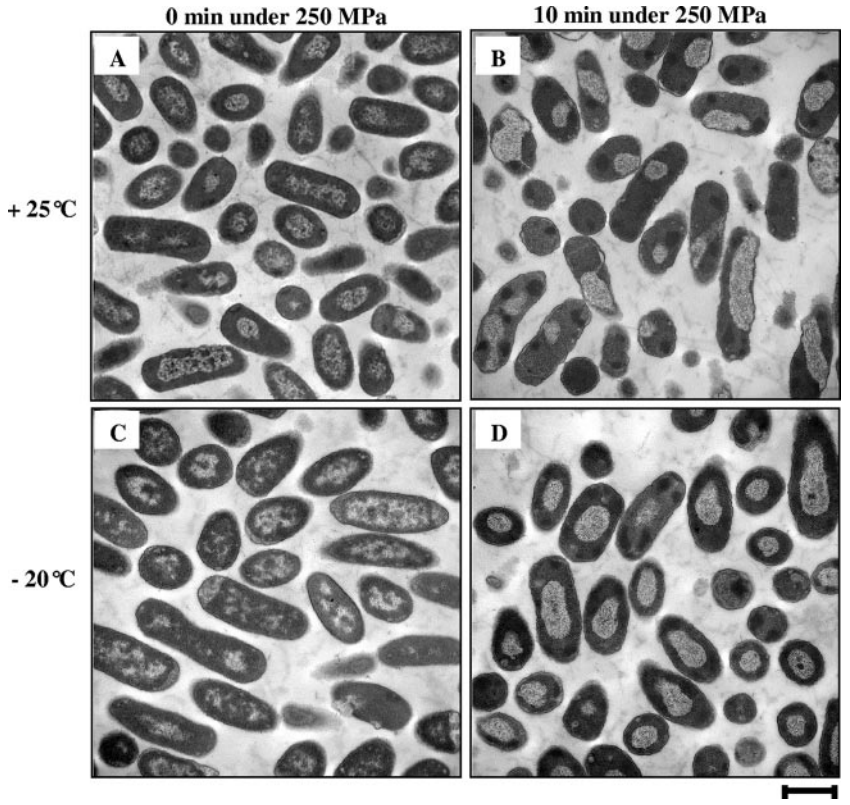

FIG. 6. TEM micrographs of *E. coli* K-12TG1 cells fixed under HHP conditions. (A and B) Cells treated at 250 MPa and +25°C for 0 min (A) and 10 min (B). (C and D) Cells treated at 250 MPa and −20°C for 0 min (C) and 10 min (D). Scale bar, 1 μm.

suggests a possible reversibility in nucleoid condensation, noticeable especially for treatments performed at −20°C. However, based on micrograph examination, protein aggregation did not seem to be reversible.

DISCUSSION

E. coli strain K-12TG1 was chosen for this study because of its ability to survive exposure to HHP treatments up to high pressure levels (above 200 MPa). Moreover, this strain showed different behaviors at room and subzero temperatures. For this reason, the pressure-mediated inactivation of *E. coli* was investigated and cells were characterized with regard to membrane integrity and ultrastructural changes to study whether the mechanisms of cell death were different at room and subzero temperatures.

Pressure-mediated cell membrane permeabilization. (i) Maintaining cells under a permeabilized state is detrimental to their survival. The assessment of membrane integrity by the exclusion of PI has been proposed by several authors (2, 8, 25). Results from our study show a low uptake of PI in cells stained after decompression, whereas a high extent of staining occurred when PI was present in the suspending medium during pressurization. We expressed these results in terms of reversible and irreversible permeabilization. Others have reported similar observations. PI staining of *L. plantarum* cells revealed only irreversible membrane damage after pressure treatments,

TABLE 2. Pressure-mediated inactivation, membrane permeabilization to PI, and structural changes in *E. coli* K12TG1 cells by HHP treatments at 250 MPa for 0 and 10 min at +25°C and −20°C[a]

Treatment conditions	% of cells with:		% Permeability to PI (±SE)		% Inactivation (inactivation in Dlog units ± SE)
	Condensed nucleoids	Aggregated proteins	Reversible	Irreversible	
250 MPa at +25°C					
0 min	94	14	6 ± 2	9 ± 2	77.61 (−0.65 ± 0.25)
10 min	96	88	16 ± 5	16 ± 3	93.24 (−1.17 ± 0.26)
250 MPa at −20°C					
0 min	95	00	23 ± 5	11 ± 2	96.28 (−1.43 ± 0.29)
10 min	92	96	37 ± 5	15 ± 3	99.96 (−3.41 ± 0.25)

[a] Structural changes were examined by TEM, and fixation was performed under pressure. The percentages of affected cells were calculated with respect to the total number of cells examined for each TEM micrograph (at least 300 cells).

resulting in an activation of greater than 5 log units (39). Pagan and Mackey (25) observed a higher level of membrane damage in *E. coli* C9490 and *E. coli* C8003 cells when PI was present during pressure treatment than when it was added after treatment. The reversible permeabilization observed in our study of *E. coli* K-12TG1 cells could be explained by the fact that membranes physically reseal after decompression to an extent where they exclude PI molecules.

It is noteworthy that the changes of membrane permeabilization with pressure and temperature were consistent with the qualitatively similar changes in cell inactivation. Indeed, if the percentages of reversible permeability and irreversible permeability are added together, HHP treatments induced higher levels of membrane permeabilization at pressures below 350 MPa and lower levels of permeabilization at pressures above 350 MPa at −20°C than at +25°C (Fig. 3). Likewise, the inactivation rate was higher at −20°C than at +25°C for pressure levels of up to 350 MPa, while the opposite trend was observed for pressure treatments of 450 and 550 MPa. Treatments at 150 and 250 MPa, which induced cell inactivation at −20°C significantly higher than that seen at +25°C, produced similar extents of irreversible permeabilization for both temperatures. Moreover, pressure treatments at −20°C induced mainly reversible permeabilization to PI (Fig. 3). Hence, cell inactivation by HHP treatments at −20°C seems closely related to reversible rather than to irreversible permeabilization. However, it should be mentioned that this correlation is qualitative rather than quantitative.

Table 2 shows that the percentage of cell membrane permeability increased with holding time under a 250-MPa treatment, especially at −20°C. This increase in PI uptake during holding time could be explained by the diffusion of PI molecules through damaged membranes and/or an increase in the extent of permeabilization. This hypothesis could also explain the mass transfer from the cytoplasm to the external medium described by some authors. Shimada et al. (33) reported leakage of internal UV-absorbing substances after pressure treatments of up to 600 MPa. Moreover, these authors reported that a mild pressure treatment of 200 MPa induced a high extent of leakage at subzero temperature but not at room temperature. Perrier-Cornet et al. (28) attributed to membrane permeabilization the leakage of intracellular solutes (Na^+, K^+, and Ca^{2+}) in yeast cells subjected to HHP treatment at 250 MPa. Using a real-time visualization device, these authors demonstrated that the average volume of yeast cells decreased to 85% of their initial volume during compression to 250 MPa. Moreover, cell volume was found to decrease steadily during holding time at 250 MPa (cells retained only 65% of their initial volume after a 15-min treatment). Shrinkage was found to be partly reversible because cells did not entirely recover their initial volume. These variations in cell volume emphasized mass transfer from the cytoplasm through the permeabilized cell membrane and were correlated with a subsequent decrease in yeast viability. Recently, Simonin et al. (34) associated time-dependent cell death during the application of a hyperosmotic stress to the maintenance of the plasma membrane in a transient state, namely, a phase separation state, that led to the leakage of cell components.

Taken together with the results of previous work (28, 34), our results lead to the suggestion that the inactivation of *E. coli* cells under combined HHP and subzero temperature occurs mainly during the time when they are transiently permeabilized. Indeed, maintaining cells in the permeabilized state under pressure is detrimental to the maintenance of homeostasis and leads ultimately to cell inactivation. At room temperature, cells are inactivated equally because of transient and permanent membrane permeabilization.

(ii) Possible mechanisms of cell membrane permeabilization. The mechanism of cell membrane permeabilization under pressure is not immediately obvious. However, it would be instructive to suggest and discuss the relevance of some hypotheses. Pressure causes closer packing of the hydrocarbon chains of membrane phospholipids, resulting in a decrease in membrane fluidity, and protein functions are influenced by the fluidity of the surrounding lipids (40). Moreover, changes in thickness and the cross-sectional area of the hydrocarbon region during phase transition would be expected to alter the environment of membrane-bound proteins in the contact surfaces of proteins and water and/or proteins and the lipid bilayer, leading to protein separation from lipid (11, 15). Kato et al. (15) suggested that pressure of up to 220 MPa causes a reversible decrease in the membrane fluidity of the lipid bilayer and a partially reversible dissociation and/or conformational change in Na^+/K^+-ATPase, allowing transmembrane tunnels to be created. For pressures above 220 MPa, protein unfolding and interface separation would lead to irreversible membrane damage (15). In addition, pressure and subzero temperature act similarly on membrane fluidity. Subzero temperature alone can induce protein destabilization (7) that can be enhanced under pressure (35). Accordingly, the high extent of reversible membrane damage observed for pressure levels of up to 350 MPa at −20°C in our study (Fig. 3) could be related to reversible changes in membrane fluidity and the conformation of membrane-bound proteins. However, the high extent of irreversible membrane permeabilization observed at +25°C and 350 MPa or above could be related to irreversible protein destabilization.

Another approach to explain membrane permeabilization could be to focus on the difference in compressibility between the cell membrane and water in the cytoplasm. Indeed, as demonstrated previously (3, 27), phospholipid vesicles with a highly compressible membrane lose part of their water content during compression because of the high compressibility of the phospholipid bilayer compared to that of the aqueous content. This water outflow did not occur in the case of vesicles with less compressible membranes. In our study, if cells behave in a way similar to that of phospholipid vesicles, the compressibility of their cytoplasm and that of their membranes will determine the severity of membrane damage induced under pressure. The involvement of the compressibility of water, considered the major constituent of the cell cytoplasm, is obvious. According to Bridgman (4), the compressibility of water increases with decreasing temperature. By contrast, the compressibility of proteins and hydrocarbon chains decreases with decreasing temperature (5). Thus, one could reasonably expect that the difference in compressibility between the cell membrane and the cytoplasm would be greater at room temperature than at subzero temperature. In turn, pressure-induced membrane damage would be more dramatic at room temperature than at

subzero temperature. This could explain the high extent of irreversible permeabilization observed at +25°C compared to −20°C (Fig. 3).

Our study points out a clear disproportion between the degree of cell inactivation and that of loss of membrane integrity. For example, treatments at 250 MPa induced more than 90% and 99.9% of cell inactivation at +25°C and −20°C, respectively (Fig. 2), although membrane permeability, irrespective of its reversibility, did not exceed 32% at +25°C and 53% at −20°C. This means that a proportion of HHP-treated cells are neither recoverable by plate counts nor stained with PI. Such cells have been described as being living but metabolically inactive (2). In addition, although these cells did not take up PI, they may be permeabilized to the extent that ions, water, and other small molecules can leak into or out of the cell cytoplasm, leading to cell death. In addition, cell death may result from the loss of metabolic functions involving ribosomes or other vital cytosolic constituents.

Pressure-mediated structural changes. (i) Could cell inactivation be correlated with pressure-mediated nucleoid condensation and protein aggregation revealed by visual examination of TEM micrographs? The evidence of TEM micrographs from our study does not show visible membrane damage that could correspond to the pressure-induced permeabilization described for Fig. 3. This leads to the suggestion that pressure treatments of up to 550 MPa are not sufficient to induce visible changes in the morphology of cells even with permeabilized membranes.

Condensation of nucleoids and aggregation of cellular proteins were obvious changes in the internal structure of treated *E. coli* cells. The condensed nucleoids were often irregularly positioned within the cell cytoplasm area. This asymmetric appearance was observed previously for *S. enterica* (21). Condensation of nucleoids was also reported for *L. monocytogenes* (21) and *L. plantarum* (41). More recently, Mañas and Mackey (22) observed nucleoid condensation of *E. coli* cells in both exponential- and stationary-phase cells stained with DAPI. In addition, our TEM micrographs showed the appearance of dense clusters that correspond to aggregated cytosolic proteins and ribosomes. Such clumps have been reported for *S. enterica* (21), *E. coli* (22), and *Leuconostoc mesenteroides* (14).

Table 1 presents an attempt to examine nucleoid condensation and protein aggregation in conjunction with microbial inactivation after different pressure treatments for 10 min. The extent of condensed nucleoids and aggregated proteins as well as the rate of cell inactivation was lowest upon treatment of 150 MPa at +25°C. Hence, it could be inferred that a pressure of 150 MPa at room temperature was not sufficiently high to cause damage to the ultrastructure of cells. The proportions of cells with condensed nucleoids were approximately the same after treatment with 250 and with 350 MPa at +25°C (83% and 89%, respectively). However, the inactivation increased to 93% for 250 MPa and increased further to more than 99% for 350 MPa. These observations are consistent with those reported by Wouters et al. (41), who observed similar extents of DNA condensation after 10-min treatments at 250 and 350 MPa, although the inactivation rates were very different (0% and 99.5% for 250 and 350 MPa, respectively). A similar discrepancy is observed between protein aggregation and microbial inactivation measured by CFU counts (Table 1).

Table 2 shows that the percentage of cells displaying protein aggregates and the inactivation rate increased with holding time under pressure, especially at −20°C. By contrast, more than 90% of cells displayed condensed nucleoids after 0- and 10-min treatments at 250 MPa at both +25°C and −20°C, despite the variation in cell inactivation as a function of temperature and holding time.

Taken together, these observations suggest that there is no absolute correlation between cell inactivation and DNA condensation/protein aggregation evaluated on the basis of visual examination of TEM micrographs.

(ii) Possible mechanisms of nucleoid condensation and protein aggregation. Pressure-induced condensation of nucleoids could be related to conformational changes in the DNA duplex under pressure. Numerous studies have focused on the conformational stability of DNA at high pressure (6, 12, 20). Given the small volume change associated with DNA transition under pressure from the helical form to the coil form, the double-stranded structure of DNA is stabilized by elevated pressure (20). Hence, the clustering of nucleoids we observed in the TEM micrographs does not necessarily indicate the denaturation of DNA. Condensation can result simply from changes in DNA packing in the cell, a phenomenon that has not been reported to be detrimental to DNA functionality. Furthermore, some authors have shown that tRNA undergoes conformational changes at a high pressure of 600 MPa but remains able to bind to ribosomes and to participate in the synthesis of polyphenylalanine in vitro (16). The difference between the appearances of nucleoids fixed under pressure and of those fixed after pressure treatment may result from the relaxation of packed DNA duplexes during decompression. In addition to the direct packing effect, pressure can act on protein-DNA complexes. Indeed, many DNA binding proteins and most enzymes that catalyze reactions with DNA require divalent metal ions. The ionic interactions between protein-DNA complexes and divalent ions are disrupted by pressure (20). Moreover, cell membrane permeabilization under pressure can lead to the leakage of divalent ions, leading to damage to the structure and the functionality of nucleoids. However, further work is needed to determine the type of damage that affects nucleoids under pressure and to enable the partial correlation between nucleoid damage and cell inactivation to be explained in a manner better than that possible based on the visual examination of micrographs.

The dense aggregated clumps observed on TEM micrographs correspond to cytosolic proteins and/or ribosomes, since they were labeled with FITC (Fig. 6). Their aggregated appearance could result from denaturation under pressure. This would be consistent with calorimetric studies showing a decrease of ribosome-associated enthalpy in cells subjected to pressure treatments (14, 24). In addition, it is well established that Mg^{2+} has a stabilizing effect on ribosome structure (37). As stated previously, ribosomes could be destabilized under pressure because of membrane permeabilization and leakage of internal Mg^{2+} content from the cell cytoplasm (24). Tables 1 and 2 do not permit an obvious correlation between aggregate formation and cell inactivation. Accordingly, a direct role of denaturation of cytosolic proteins and/or ribosomes in the cell death process remains questionable. Further work is needed to characterize more precisely the nature of proteins

contained in the aggregates and to clarify their involvement in cell inactivation.

With respect to the data presented in Tables 1 and 2, the extent of protein aggregation in cells fixed before decompression was not very different from that observed for cells fixed after decompression. Moreover, there is no noticeable difference in the appearances of protein clumps fixed before and after decompression. However, it could be hypothesized that reversal of protein aggregation does occur but could not be discriminated based on visual examination of TEM micrographs.

Conclusion. Our study supports the widely established view that membrane damage is a key mechanism involved in the inactivation of cells by high pressure. The nature of membrane damage was found to depend on the temperature of pressurization. Indeed, pressure treatments at subzero temperature induced mainly reversible permeabilization, while both reversible and irreversible permeabilization occurred at room temperature. However, the correlation between cell inactivation and membrane permeabilization is qualitative rather than quantitative. Accordingly, other mechanisms, such as loss of metabolic functions involving ribosomes or other vital cytosolic constituents, should not be neglected.

TEM results showed obvious changes in nucleoids and cytosolic proteins of cells fixed after decompression. A novel technique was used to mix fixation reagents with the cell suspension under HHP and subzero-temperature conditions. This technique made it possible to demonstrate the partial reversibility of nucleoid condensation under pressure. However, visual examination of TEM micrographs was based on the "all or nothing" rule, which did not allow an absolute correlation of structural changes with cell inactivation. Further work should be undertaken with a view to better elucidating the involvement in cell inactivation of pressure-induced damage to nucleoids and proteins.

ACKNOWLEDGMENTS

Marwen Moussa was supported by a grant provided by the Tunisian Mission of University Study in France.

We thank Frank Menetrier, Josette Rollot, and Jeannine Lherminier for their skillful technical assistance with TEM.

REFERENCES

1. **Ananta, E., V. Heinz, and D. Knorr.** 2004. Assessment of high pressure induced damage on *Lactobacillus rhamnosus* GG by flow cytometry. Food Microbiol. **21:**567–577.
2. **Arroyo, G., P. D. Sanz, and G. Prestamo.** 1999. Response to high-pressure, low-temperature treatment in vegetables: determination of survival rates of microbial populations using flow cytometry and detection of peroxidase activity using confocal microscopy. J. Appl. Microbiol. **86:**544–556.
3. **Beney, L., J. M. Perrier-Cornet, M. Hayert, and P. Gervais.** 1997. Shape modification of phospholipid vesicles induced by high pressure: influence of bilayer compressibility. Biophys. J. **72:**1258–1263.
4. **Bridgman, P. W.** 1912. Water, in the liquid and five solid forms under pressure. Proc. Am. Acad. Arts Sci. **47:**441–558.
5. **Chalikian, T. V., A. P. Sarvazyan, and J. B. Kenneth.** 1994. Hydration and partial compressibility of biological compounds. Biophys. Chem. **51:**89–109.
6. **Chalikian, T. V., J. Volker, A. R. Srinivasan, W. K. Olson, and K. J. Breslauer.** 1999. The hydration of nucleic acid duplexes as assessed by a combination of volumetric and structural techniques. Biopolymers **50:**459–471.
7. **Franks, F.** 1995. Protein destabilization at low temperatures. Adv. Protein Chem. **46:**105–139.
8. **Ganzle, M. G., and R. F. Vogel.** 2001. On-line fluorescence determination of pressure mediated outer membrane damage in *Escherichia coli*. Syst. Appl. Microbiol. **24:**477–485.
9. **Hashizume, C., K. Kimura, and R. Hayashi.** 1995. Kinetic analysis of yeast inactivation by high pressure treatment at low temperatures. Biosci. Biotechnol. Biochem. **59:**1455–1458.
10. **Hayakawa, K., Y. Ueno, S. Kawamura, T. Kato, and R. Hayashi.** 1998. Microorganism inactivation using high-pressure generation in sealed vessels under sub-zero temperature. Appl. Microbiol. Biotechnol. **50:**415–418.
11. **Hayashi, R.** 2002. High pressure in bioscience and biotechnology: pure sciences encompassed in pursuit of value. Biochim. Biophys. Acta **1595:**397–399.
12. **Heden, C. G., T. Lindahl, and I. Toplin.** 1964. The stability of deoxyribonucleic acid solutions under high pressure. Acta Chem. Scand. **5:**1150–1156.
13. **Helander, I. M., and T. Mattila-Sandholm.** 2000. Fluorimetric assessment of gram-negative bacterial permeabilization. J. Appl. Microbiol. **88:**213–219.
14. **Kaletunç, G., J. Lee, H. Alpas, and F. Bozoglu.** 2004. Evaluation of structural changes induced by high hydrostatic pressure in *Leuconostoc mesenteroides*. Appl. Environ. Microbiol. **70:**1116–1122.
15. **Kato, M., R. Hayashi, T. Tsuda, and K. Taniguchi.** 2002. High pressure-induced changes of biological membrane. Study on the membrane-bound Na+/K+-ATPase as a model system. Eur. J. Biochem. **269:**110–118.
16. **Krzyzaniak, A., P. Salanski, T. Twardowski, J. Jurczak, and J. Barciszewski.** 1998. tRNA aminoacylated at high pressure is a correct substrate for protein biosynthesis. Biochem. Mol. Biol. Int. **45:**489–500.
17. **Ludwig, H., C. Bieler, K. Hallbauer, and W. Scigalla.** 1992. Inactivation of microorganisms by hydrostatic pressure, p. 25–32. *In* C. Balny, R. Hayashi, K. Heremans, and P. Masson (ed.), High pressure and biotechnology. John Libbey and Co., Ltd., London, England.
18. **Luscher, C., A. Balasa, A. Frohling, E. Ananta, and D. Knorr.** 2004. Effect of high-pressure-induced ice I-to-ice III phase transitions on inactivation of *Listeria innocua* in frozen suspension. Appl. Environ. Microbiol. **70:**4021–4029.
19. **Macdonald, A. G.** 1984. The effects of pressure on the molecular structure and physiological functions of cell membranes. Phil. Trans. R. Soc. Lond. B **304:**47–68.
20. **Macgregor, R. B.** 2002. The interactions of nucleic acids at elevated hydrostatic pressure. Biochim. Biophys. Acta **1595:**266–276.
21. **Mackey, B. M., K. Forestière, N. S. Isaacs, R. Stenning, and B. Brooker.** 1994. The effect of high hydrostatic pressure on *Salmonella thompson* and *Listeria monocytogenes* examined by electron microscopy. Lett. Appl. Microbiol. **19:**429–432.
22. **Mañas, P., and B. M. Mackey.** 2004. Morphological and physiological changes induced by high hydrostatic pressure in exponential- and stationary-phase cells of *Escherichia coli*: relationship with cell death. Appl. Environ. Microbiol. **70:**1545–1554.
23. **Moussa, M., J. M. Perrier-Cornet, and P. Gervais.** 2006. Synergistic and antagonistic effects of combined subzero temperature and high pressure on inactivation of *Escherichia coli*. Appl. Environ. Microbiol. **72:**150–156.
24. **Niven, G. W., C. A. Miles, and B. M. Mackey.** 1999. The effects of hydrostatic pressure on ribosome conformation in *Escherichia coli*: an in vivo study using differential scanning calorimetry. Microbiology **145:**419–425.
25. **Pagan, R., and B. Mackey.** 2000. Relationship between membrane damage and cell death in pressure-treated *Escherichia coli* cells: differences between exponential- and stationary-phase cells and variation among strains. Appl. Environ. Microbiol. **66:**2829–2834.
26. **Park, S. W., K. H. Sohn, J. H. Shin, and H. J. Lee.** 2001. High hydrostatic pressure inactivation of *Lactobacillus viridescens* and its effects on ultrastructure of cells. Int. J. Food Sci. Technol. **36:**775–781.
27. **Perrier-Cornet, J. M., K. Baddouj, and P. Gervais.** 2005. Pressure-induced shape change of phospholipid vesicles: implications of compression and phase transition. J. Membr. Biol. **204:**101–107.
28. **Perrier-Cornet, J. M., M. Hayert, and P. Gervais.** 1999. Yeast cell mortality related to a high-pressure shift: occurrence of cell membrane permeabilization. J. Appl. Microbiol. **87:**1–7.
29. **Perrier-Cornet, J. M., S. Tapin, S. Gaeta, and P. Gervais.** 2005. High-pressure inactivation of *Saccharomyces cerevisiae* and *Lactobacillus plantarum* at subzero temperatures. J. Biotechnol. **115:**405–412.
30. **Picart, L., E. Dumay, J. P. Guiraud, and C. Cheftel.** 2005. Combined high pressure-subzero temperature processing of smoked salmon mince: phase transition phenomena and inactivation of *Listeria innocua*. J. Food Eng. **68:**43–56.
31. **Ritz, M., M. Freulet, N. Orange, and M. Federighi.** 2000. Effects of high hydrostatic pressure on membrane proteins of *Salmonella typhimurium*. Int. J. Food Microbiol. **55:**115–119.
32. **Shen, T., G. Urrutia Benet, S. Brul, and D. Knorr.** 2005. Influence of high-pressure-low-temperature treatment on the inactivation of *Bacillus subtilis* cells. Innov. Food Sci. Emerg. Technol. **6:**271–278.
33. **Shimada, S., M. Andou, N. Naito, N. Yamada, M. Osumi, and R. Hayashi.** 1993. Effects of hydrostatic pressure on the ultrastructure and leakage of internal substances in the yeast *Saccharomyces cerevisiae*. Appl. Microbiol. Biotechnol. **40:**123–131.
34. **Simonin, H., L. Beney, and P. Gervais.** Cell death induced by mild physical perturbations could be related to transient plasma membrane modifications. J. Membr. Biol., in press.

35. **Smeller, L.** 2002. Pressure-temperature phase diagrams of biomolecules. Biochim. Biophys. Acta **1595:**11–29.
36. **Sonoike, K., T. Setoyama, Y. Kuma, and S. Kobayashi.** 1992. Effect of pressure and temperature on the death rates of *Lactobacillus casei* and *Escherichia coli*, p. 297–301. *In* C. Balny, R. Hayashi, K. Heremans, and P. Masson (ed.), High pressure and biotechnology. John Libbey and Co., Ltd., London, England.
37. **Stahli, C., and H. Noll.** 1977. Structural dynamics of bacterial ribosomes. VI. Denaturation of active ribosomes by Mg^{2+} dependent conformational transitions. Mol. Gen. Genet. **153:**159–168.
38. **Takahashi, K.** 1992. Sterilization of microorganisms by hydrostatic pressure at low temperature, p. 303–307. *In* C. Balny, R. Hayashi, K. Heremans, and P. Masson (ed.), High pressure and biotechnology. John Libbey and Co., Ltd., London, England.
39. **Ulmer, H. M., M. G. Ganzle, and R. F. Vogel.** 2000. Effects of high pressure on survival and metabolic activity of *Lactobacillus plantarum* TMW1.460. Appl. Environ. Microbiol. **66:**3966–3973.
40. **Ulmer, H. M., H. Herberhold, S. Fahsel, M. G. Ganzle, R. Winter, and R. F. Vogel.** 2002. Effects of pressure-induced membrane phase transitions on inactivation of HorA, an ATP-dependent multidrug resistance transporter, in *Lactobacillus plantarum*. Appl. Environ. Microbiol. **68:**1088–1095.
41. **Wouters, P., E. Glassker, and J. P. P. M. Smelt.** 1998. Effects of high pressure on inactivation kinetics and events related to proton efflux in *Lactobacillus plantarum*. Appl. Environ. Microbiol. **64:**509–514.